THE JOURNAL OF BIOLOGICAL CHEMISTRY
Vol. 277, No. 32, Issue of August 9, pp. 28641–28647, 2002
Printed in U.S.A.

BRCA1 Facilitates Microhomology-mediated End Joining of DNA Double Strand Breaks*

Received for publication, January 23, 2002, and in revised form, May 21, 2002
Published, JBC Papers in Press, May 30, 2002, DOI 10.1074/jbc.M200748200

Qing Zhong‡, Chi-Fen Chen, Phang-Lang Chen, and Wen-Hwa Lee§

From the Department of Molecular Medicine, Institute of Biotechnology, University of Texas Health Science Center at San Antonio, San Antonio, Texas 78245

BRCA1 is critical for the maintenance of genomic stability, in part through its interaction with the Rad50·Mre11·Nbs1 complex, which occupies a central role in DNA double strand break repair mediated by nonhomologous end joining (NHEJ) and homologous recombination. BRCA1 has been shown to be required for homology-directed recombination repair. However, the role of BRCA1 in NHEJ, a critical pathway for the repair of double strand breaks and genome stability in mammalian cells, remains elusive. Here, we established a pair of mouse embryonic fibroblasts (MEFs) derived from 9.5-day-old embryos with genotypes *Brca1*$^{+/+}$:*p53*$^{-/-}$ or *Brca1*$^{-/-}$:*p53*$^{-/-}$. The *Brca1*$^{-/-}$:*p53*$^{-/-}$ MEFs appear to be extremely sensitive to ionizing radiation. The contribution of BRCA1 in NHEJ was evaluated in these cells using three different assay systems. First, transfection of a linearized plasmid in which expression of the reporter gene required precise end joining indicated that *Brca1*$^{-/-}$ MEFs display a moderate deficiency when compared with *Brca1*$^{+/+}$ cells. Second, using a retrovirus infection assay dependent on NHEJ, a 5–10-fold reduction in retroviral integration efficiency was observed in *Brca1*$^{-/-}$ MEFs when compared with the *Brca1*$^{+/+}$ MEFs. Third, *Brca1*$^{-/-}$ MEFs exhibited a 50–100-fold deficiency in microhomology-mediated end-joining activity of a defined chromosomal DNA double strand break introduced by a rare cutting endonuclease I-*Sce*I. These results provide evidence that Brca1 has an essential role in microhomology-mediated end joining and suggest a novel molecular basis for its caretaker role in the maintenance of genome integrity.

Inactivation of the breast cancer susceptibility gene, *BRCA1*, accounts for a significant portion of familial breast cancer (1, 2). Chromosome aneuploidy has been reported in human breast cancer cells, HCC1937, which contain a C-terminal truncated BRCA1 (3). Similarly, murine fibroblasts containing a deletion within exon 11 of BRCA1 display extensive chromosomal abnormality (4). Both Brca1-deficient murine and human cells have been shown to be sensitive to DNA-damaging agents, including ionizing radiation (5–7), suggesting that BRCA1 may play an essential role in DNA double strand break (DSB)[1] repair. DSBs can be repaired through homologous recombination (HR) or nonhomologous end joining (NHEJ) to ensure the maintenance of genome integrity in eukaryotic organisms (8). More significantly, deficiencies in the mammalian NHEJ pathway can lead to an increase in the frequency of chromosomal translocations and the rate of neoplastic transformation (9–13), thus emphasizing the importance of this DSB repair pathway in the maintenance of genome integrity.

BRCA1 binds to the Rad50·Mre11·Nbs1 complex and can form radiation-induced foci with this complex (14). The yeast counterpart of this complex, Rad50·Mre11·Xrs2, is required for both NHEJ and HR (15). BRCA1 has been implicated in homology-based recombination repair (16). In the study described by Moynahan *et al.* (16), a reporter substrate containing two differentially mutated neomycin phosphotransferase gene (*neo*) placed in tandem, with one harboring an I-*Sce*I cleavage site, was integrated into the genome of both wild-type or Brca1 exon 11 deleted embryonic stem (ES) cells. Upon expression of the I-*Sce*I endonuclease, ES cells containing the Brca1 exon 11 deleted mutant, but not wild-type Brca1, showed a deficiency in intra- and interchromosomal recombination (16). Interestingly, these Brca1 mutant cells showed a slight increase in nonhomologous repair processes characterized by nucleotide deletion or addition (16). However, neither precise end joining, which may account for nearly 60% of the end-joining events in the I-*Sce*I-inducible DNA DSB repair (17), nor a microhomology-mediated end-joining activity that may recover a functional *neo* gene independent of gene conversion was taken into consideration in this assay system (16). Moreover, it is likely that repair by HR contributes much more than NHEJ in ES cells because of their relatively short cell cycle duration (18). Thus, the potential role of BRCA1 in NHEJ may not be revealed by this reported assay system (16). In BRCA1-deficient HCC1937 cells, a much slower rate and less extensive amount of DSB repair, as measured by pulse field gel electrophoresis (PFGE) at 6 h after ionizing irradiation, has been observed as compared with the same cells expressing wild-type BRCA1 protein (19). The altered kinetics of the PFGE assay primarily reflects the inefficiency of chromosomal break rejoining, which is commonly observed in mutant cells deficient in NHEJ mutant but not in HR (20). This finding, albeit circumstantial, suggests that BRCA1 may participate in NHEJ.

To address the potential role of BRCA1 in NHEJ, we utilized three independent *in vivo* approaches demonstrating that BRCA1 promotes NHEJ mediated by microhomology. Trans-

* This work was supported by grants from the National Institutes of Health (CA 85605 to P.-L. C. and CA 81020, CA58183, and CA30195 to W.-H. L.). The costs of publication of this article were defrayed in part by the payment of page charges. This article must therefore be hereby marked "*advertisement*" in accordance with 18 U.S.C. Section 1734 solely to indicate this fact.

‡ Supported by a postdoctoral training grant from the United States Army Medical Research and Materiel Command under DAMD17-00-1-0457.

§ To whom correspondence should be addressed: Dept. of Molecular Medicine, Institute of Biotechnology, University of Texas Health Science Center at San Antonio, 15355 Lambda Dr., San Antonio, TX 78245. Tel.: 210-567-7351; Fax: 210-567-7377; E-mail: leew@ uthscsa.edu.

[1] The abbreviations used are: DSB, double strand break; HR, homologous recombination; NHEJ, nonhomologous end joining; m.o.i., multiplicity(s) of infection; ES cells, embryonic stem cells; MEF, mouse embryonic fibroblast; GFP, green fluorescent protein.

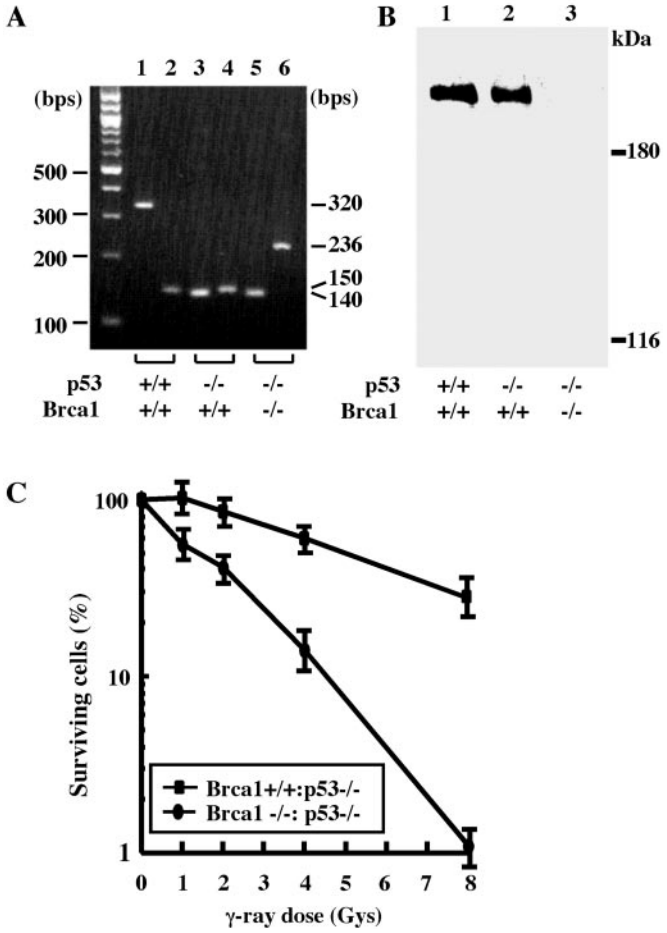

FIG. 1. *A*, genotyping of MEFs. The methods for genotyping wild-type and mutant *p53* or *Brca1* are described under "Materials and Methods." The resulting sizes of the different PCR products serving as diagnostic markers for the different alleles are as follows: 320 bp for wild-type *p53*, 140 bp for mutated *p53*, 150 bp for wild-type *Brca1*, and 236 bp for the mutated *Brca1* allele. *Lanes 1*, *3*, and *5* were PCR products derived from the *p53* locus. *Lanes 2*, *4*, and *6* were derived from the *Brca1* locus. Genomic DNA used in *lanes 1* and *2* was extracted from $Brca1^{+/+}$:$p53^{+/+}$, in *lanes 3* and *4* from $Brca1^{+/+}$:$p53^{-/-}$, and in *lanes 5* and *6* from $Brca1^{-/-}$:$p53^{-/-}$. *B*, expression of Brca1 in wild-type, $Brca1^{+/+}$:$p53^{-/-}$, and $Brca1^{-/-}$:$p53^{-/-}$ MEFs. Cell lysates were prepared from these MEFs for protein analysis by immunoprecipitation followed by Western blotting using anti-mouse Brca1 antibody. In $Brca1^{-/-}$:$p53^{-/-}$ MEFs, the full-length Brca1 protein was not detected. *C*, $Brca1^{-/-}$:$p53^{-/-}$ MEFs are hypersensitive to γ-irradiation. $Brca1^{+/+}$:$p53^{-/-}$and $Brca1^{-/-}$:$p53^{-/-}$ MEFs were either exposed to different doses of γ-irradiation as indicated or mock-exposed. Surviving colonies were counted 10 days later. The results shown represent the mean ± standard deviation of three independent experiments.

fection of a linearized plasmid in which expression of the reporter gene required precise end joining indicated that $Brca1^{-/-}$ MEFs display a moderate deficiency when compared with $Brca1^{+/+}$ MEFs. Further, Brca1 promotes efficient retroviral infection, which depends on an intact NHEJ pathway. Most importantly, Brca1-deficient MEFs exhibit severely impaired end-joining activity mediated by microhomology in response to I-*Sce*I restriction endonuclease induced chromosomal double-stranded DNA break. These results support a role for Brca1 in NHEJ and provide a biochemical basis for the caretaker function of BRCA1 in the maintenance of genome integrity.

MATERIALS AND METHODS

Mouse Embryonic Fibroblast

To prepare $Brca1^{-/-}$:$p53^{-/-}$ and $p53^{-/-}$ mouse embryonic fibroblasts (MEFs), $Brca1^{+/-}$ mice derived from a Brca1-ko(o)3 targeted ES clone (21) were crossed with $p53^{-/-}$ mice (Jackson Laboratory). Brca1-ko(o)3 contained a neo cassette in the opposite orientation within Brca1 exon 11. The resultant F_1 $Brca1^{+/-}$:$p53^{-/-}$ mice were then crossed with each other, and embryos about 9.5 days old were used to prepare MEFs as described (22).

PCR Genotyping

Primers for genotyping *Brca1* were as described (21). In short, a 236-bp PCR product was the diagnostic indicator of the targeted *Brca1* allele, and a 150-bp product was diagnostic of the wild-type allele. For the targeted *p53* allele, a 140-bp PCR product was generated using a sense oligonucleotide, 5′-AGTTCGAGGCCATCTCTGACTACAC-3′ and an antisense oligonucleotide, 5′-CTGTGCTCTAGTAGCTTTACGGAGC-3′, within the *PolII* promoter. A 320-bp PCR product was diagnostic of the wild-type allele using the same sense oligonucleotide and an antisense oligonucleotide, 5′-GAGGGGAGGAGAGTACTGGAAGAGA-3′, within exon 5 of the *p53* gene (23).

Irradiation and Clonogenic Survival Assay

$Brca1^{-/-}$:$p53^{-/-}$ and $p53^{-/-}$ MEFs were seeded in identical plates at 4000 cells/6-cm dish in regular medium for 24 h. Cells were then irradiated with 0, 1, 2, 4, and 8 grays using a Mark I, model 68A, irradiator. After 14 days, the colonies were fixed and stained with 2% methylene blue in 50% ethanol and then counted.

Adenovirus I-SceI Construct

pPGK3XNLS-I-*Sce*I was kindly provided by P. Berg and G. Donoho (Stanford University). The entire I-*Sce*I DNA fragment was digested with *Sal*I and *Pst*I and cloned into the pBluescript vector, referred to as pBSK-I-*Sce*I. This plasmid was then digested with *Not*I and *Xho*I to release I-*Sce*I and inserted into the AdTrack.CMV plasmid (a gift from B. Vogelstein) (24) to form the AdTrack-CMV-I-*Sce*I plasmid. The adenovirus was then produced following the protocol as described (24).

Mouse Brca1 Antibodies, Immunoprecipitation, and Western Blotting

Mouse Brca1 cDNA-encoded amino acids 788–1135 was translationally fused to glutathione *S*-transferase in-frame, and the bacterially generated fusion protein derived from this construct was used as an antigen for producing mouse polyclonal antisera. Immunoprecipitation and Western blotting were performed as described previously (14).

Transfection and Luciferase Activity Assay

pGL2 plasmid (Promega) was completely linearized by restriction endonuclease *Hin*dIII or *Eco*RI and confirmed by agarose gel electrophoresis. The linearized DNA was subjected to phenol/chloroform extraction, ethanol-precipitated, and dissolved in sterilized water. DNA was then transfected into cells with Fugene 6 following the procedures described by the supplier (Roche Molecular Biochemicals). The transfected cells were harvested and assayed for luciferase activity as described (22).

Retroviral Infection Assay

MEFs were plated at 5×10^5/10-cm dish and infected with a 477H recombinant retrovirus carrying a hygromycin resistance gene for 24 h (25). The infected cells were then selected by hygromycin (200 μg/ml) for 10–14 days. The resulting hygromycin-resistant colonies were counted on three plates for each infection titer, and the experiments were repeated three times.

Chromosomal DNA End-joining Assay

Substrate Construction—pBSK-S1hygro was constructed by inserting an endonuclease I-*Sce*I recognition sequence into the unique *Nco*I site of pBSK-PGKhygro as described below. The *Nco*I site was filled in using Klenow fragment and ligated with an 18-bp I-*Sce*I recognition sequence of 5′-CATGATTACCCTGTTTATCCCTA-3′. A DNA cassette containing puromycin resistance gene driven by the SV40 T antigen promoter was then inserted into pBSK-S1hygro. The entire *S1hygro* with puromycin gene was propagated as a plasmid, and the plasmid DNA was then transfected into MEFs followed by a selection with 2 μg/ml puromycin. Cell clones that contained one to two copies of *S1hygro* identified by genomic DNA blotting analysis were selected for further experiments.

S1hygro Retrovirus—The entire *S1hygro* with puromycin gene was released and inserted into an engineered murine leukemia virus (MuLV)-based retroviral vector. The *S1hygro* virus, produced by transfecting the constructed viral vector DNA into Phoenix Ampho packag-

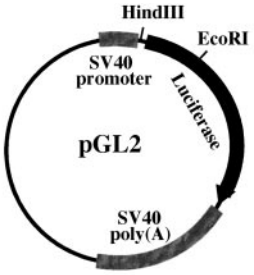

Cell lines	Relative end-joining efficiency	
	HindIII/uncut	EcoRI/uncut
p53-/-Brca1+/+	29.0 ± 2.4%	11.9 ± 0.6%
p53-/-Brca1-/-	31.6 ± 0.1%	7.1 ± 0.2%

FIG. 2. **Plasmid end-joining assay.** The pGL2-control plasmid as illustrated contains two unique restriction sites, *Hin*dIII and *Eco*RI. The relative end-joining efficiency was calculated by comparing luciferase activity expressed in MEFs transfected with *Hin*dIII- or *Eco*RI-digested DNA with that of the uncut plasmid. The results shown were from three independent transfection experiments.

ing cells as described (26), was used to infect MEFs. MEF clones grown out from the selection of puromycin (2 μg/ml) and containing a single copy of proviral DNA of *S1hygro* substrate were used for the end-joining experiments.

Microhomology-mediated End-joining Assay—MEF clones containing a single copy of *S1hygro* substrate were transfected with pPGK3Xnls-I-*Sce*I or infected with I-*Sce*I adenovirus to express I-*Sce*I endonuclease that cleaves the I-*Sce*I site at the proviral hygromycin DNA. The cells were subsequently selected in medium with hygromycin (200 μg/ml) for 14 days, and the hygromycin-resistant colonies were counted. To examine whether these resistant colonies arose from the microhomology-mediated end-joining repair, genomic DNA was extracted for PCR analysis using the primers hygro-4 (5′-CCTGCGGGTAAATAGCTGCGCCGATG-3′) and hygro-5 (5′-CATACAAGC CAACCACGGCCTCCAG-3′) within the hygromycin resistance gene to generate a 595-bp DNA fragment that included the original inactivated *Nco*I and I-*Sce*I sites. Recovery of the *Nco*I site by microhomology-mediated end joining was indicated by the cleavage of the 595-bp fragment into a 379- and a 216-bp fragment following *Nco*I restriction enzyme digestion.

RESULTS

Brca1 Null MEFs Are Hypersensitive to Ionizing Irradiation—Previously, mice carrying a mutated *Brca1* allele with a small 5′ portion of exon 11 replaced by a neomycin gene were generated and shown to be viable (21). However, mice with both alleles mutated were embryonic lethal at postnatal days 5–7 (22). This phenotype was much more severe when compared with mice carrying both alleles of *Brca1* deleted for exon 11, which displayed an extended embryonic life span (4, 27, 28). Therefore, the MEFs derived from our *Brca1* knock-out mouse may be useful in exploring the full function of the *Brca1* gene. Because the mutant Brca1 embryos died too early to generate MEFs, survival of $Brca1^{-/-}$ mutant embryos could be extended with the ablation of the p53 gene (4, 29). MEFs with $Brca1^{-/-}$:$p53^{-/-}$ or $p53^{-/-}$ genotype were then established from E9.5 embryos (Fig. 1*A*) derived from a cross of $Brca1^{+/-}$:$p53^{-/-}$ mice (21). Protein analysis by immunoprecipitation followed by Western blotting revealed no full-length BRCA1 protein in these $Brca1^{-/-}$:$p53^{-/-}$ MEFs (Fig. 1*B*). Importantly, the Brca1-deficient MEFs exhibited hypersensitivity to γ-irradiation when compared with the $p53^{-/-}$ MEFs (Fig. 1*C*). The degree of γ-irradiation sensitivity of this $Brca1^{-/-}$:$p53^{-/-}$ MEF is greater than mouse embryonic stem cells or MEFs carrying a Brca1 exon 11 spliced variant (5, 6).

Brca1 Affects Precise End Joining rather than Overall End Joining—To examine the potential contribution of Brca1 in DSB repair, the established Brca1-deficient MEFs were used in a plasmid end-joining assay utilizing transient transfection of a linearized pGL2 plasmid harboring a luciferase reporter gene. If the reporter plasmid was linearized with restriction endonuclease *Hin*dIII, which cleaved at the linker region between promoter and coding sequence, any end-joining activity with small deletion or insertion would not affect the expression of the luciferase gene and could be considered an overall end-joining activity. However, if the reporter plasmid was digested with *Eco*RI at the luciferase coding region, only precise end joining would restore the original sequence (Fig. 2). Repair efficiency was calculated from the luciferase activities of linearized reporter constructs compared with that of the intact plasmid. We observed no difference in the overall end-joining activity between the $Brca1-/-$:$p53^{-/-}$ *and* $p53^{-/-}$ MEFs, but Brca1-deficient MEFs exhibited about a 50% reduction in precise end-joining activity (Fig. 2).

BRCA1 Is Required for Efficient Retroviral Infection Mediated by NHEJ—It has been reported that cells deficient in proteins involved in NHEJ show a reduced efficiency of retroviral infection (30, 31), suggesting that NHEJ is critical for the resolution of DNA DSBs that arise during retroviral infection. The first report suggested that NHEJ is required for retroviral DNA integration that proceeds through the repair of gapped intermediates arising from the linkage of viral and host cell DNA in an early reaction catalyzed by the viral integrase protein. The repair of gapped intermediates, which consist of nonjoined viral DNA 5′ ends, results in a 4–6-base pair repeat of host cell DNA flanking each proviral end (30). The second report demonstrated that cells with mutated NHEJ proteins suffer a high level of cell death upon retroviral infection (31) and proposed that, instead of being involved in an early step of retroviral integration, the NHEJ proteins are required to circularize the linear viral DNA to conceal the exposed DSBs to prevent subsequent apoptosis (31). In either case, NHEJ appears to be essential for retroviral infection.

Based on these findings, we decided to examine the efficiency of retroviral infection in the Brca1 deficient cells. Following infection with a retrovirus, 477H, carrying a hygromycin resistance gene (*Hygro*^{r}), the frequency of hygromycin-resistant colonies was found to be 5–10-fold lower in the $Brca1^{-/-}$:$p53^{-/-}$ MEFs as compared with the matched $Brca1^{+/+}$:$p53^{-/-}$ MEFs (Fig 3, *A* and *B*). Similarly, a 3–5-fold reduction in the number of hygromycin-resistant colonies was also observed in infected $Ku80^{-/-}$:$p53^{-/-}$ MEFs (13) as compared with $Ku80^{+/-}$:$p53^{-/-}$ MEFs (Fig. 3*B*). These results are consistent with the notion that DNA end-joining activity is significantly reduced in Brca1-deficient cells.

Brca1 Promotes Nonhomologous End joining of Chromosomal DSBs—In an attempt to further substantiate the contribution of Brca1 in NHEJ, we modified a DSB repair assay system (32) that permitted us to measure the frequency of NHEJ at a defined chromosomal DSB. For this purpose, we established $p53^{-/-}$ and $Brca1^{-/-}$:$p53^{-/-}$ MEF cell lines that carried a single integrated copy of a defined DSB repair substrate. This substrate, *S1hygro*, contained one copy of the hygromycin resistance gene (*Hygro*^{r}) carrying an 18-base pair recognition sequence for the rare cutting restriction endonuclease I-*Sce*I inserted into a naturally occurring *Nco*I site (Fig. 4), therefore leaving 4 bp of CATG microhomologies (residual *Nco*I site) flanking the I-*Sce*I site (Fig. 4*A*). This modification resulted in the inactivation of the hygromycin resistance gene. However, upon I-*Sce*I endonuclease cleavage, hygromycin-resistant activity could be restored, if this defined DSB was resected to a point at which the CATG microhomologies could be detected, and rejoined to restore the *Nco*I site, thereby

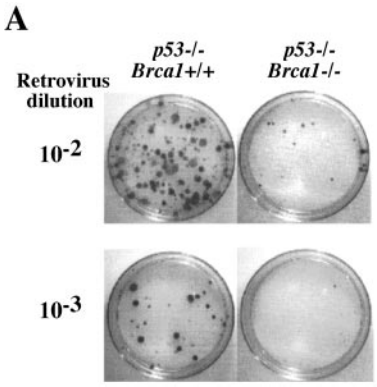

B

Number of Hygro^r colonies		
	Retrovirus dilution	
Cell lines	10^{-2}	10^{-3}
p53-/-Ku+/-	544 ± 21	110 ± 18
p53-/-Ku+/-	557 ± 21	102 ± 3
p53-/-Ku-/-	171 ± 18	37 ± 7
p53-/-Ku-/-	142 ± 39	21 ± 6
p53-/-Brca1+/+	456 ± 21	77 ± 39
p53-/-Brca1-/-	44 ± 7	14 ± 3

1x10^6 cells were used in each experiment.

FIG. 3. **Retroviral infection assay.** *A*, *Brca1*$^{+/+}$:*p53*$^{-/-}$and *Brca1*$^{-/-}$:*p53*$^{-/-}$ MEFs were plated at 5 × 10^5/100-mm dish and infected for 24 h with the indicated dilutions of virus 477H carrying a hygromycin resistance gene. Cells were selected with hygromycin (200 μg/ml) for 10–14 days and stained with methylene blue. Representative plates are shown. *B*, efficiency of retroviral DNA infection in distinct MEFs. The number of hygromycin-resistant colonies was counted from three plates for each assay, and each experiment was repeated three times.

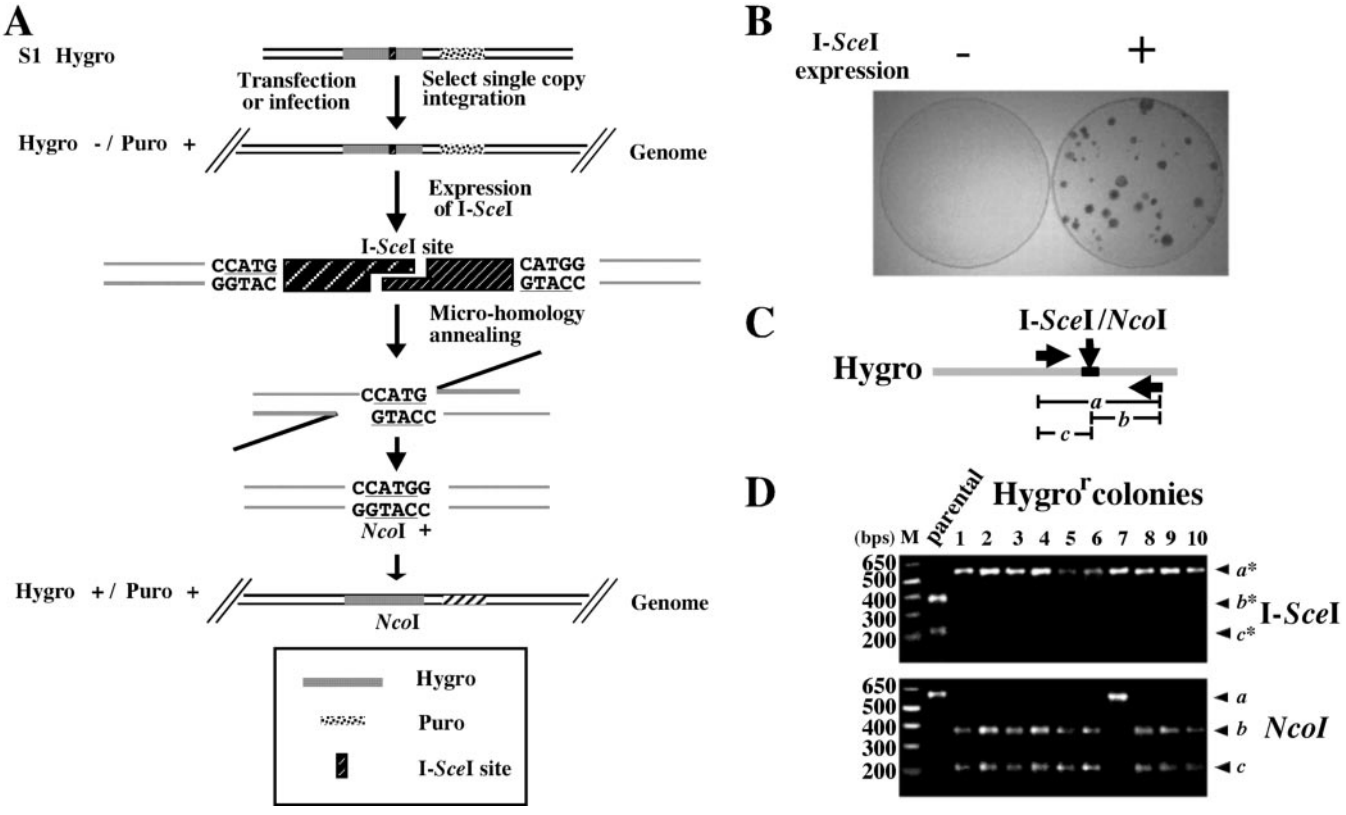

FIG. 4. **Design and analysis of the microhomology-mediated end-joining assay.** *A*, illustration of the scheme for I-*Sce*I-induced chromosomal end-joining reaction using the CATG microhomology sequence of the inactivated *Nco*I site. *B*, expression of I-*Sce*I in *p53*$^{-/-}$ MEFs promotes NHEJ-mediated repair of the *S1hygro* substrate. Two identical plates of MEFs with a single integrated copy of *S1hygro* substrate were transfected with an I-*Sce*I expression vector (+) or control vector (−). The dishes were fixed and stained with methylene blue. Representative dishes are shown. *C*, physical analysis of NHEJ products. PCR reaction using a pair of primers within the hygromycin gene generates a DNA fragment of ~573–595 bp (*a*). If this fragment contained a recovered *Nco*I site, digestion with restriction enzyme *Nco*I would produce two fragments of 368 (*b*) and 205 bp (*c*), respectively. *D*, physical analysis of genomic DNA extracted from both hygromycin-resistant clones (hygro^r) and parental cells containing *S1hygro*. PCR reactions were performed using primers flanking the I-*Sce*I or *Nco*I site as shown in *panel C*. Upon I-*Sce*I endonuclease digestion, the PCR product (*a*) from the parental clone cleaved into two fragments, *b** (379 bp) and *c** (216 bp), indicating the intact I-*Sce*I site. However, I-SceI failed to cleave the PCR fragments (*a**) from the 10 hygromycin-resistant clones (*lanes 1–10*). Conversely, upon *Nco*I restriction digestion, 9 of 10 clones (except *lane 7*) gave rise to the *b* and *c* fragments, which were not seen in the parental clone. Clone 7 apparently went through a different repair mechanism because it lost both the I-*Sce*I and *Nco*I sites but kept hygromycin resistance.

generating an intact hygromycin resistance gene (Fig. 4*A*). The original sequence was unlikely to be restored by homologous recombination due to the absence of homologous sequence. Importantly, this type of NHEJ repair promoted by an I-*Sce*I-induced DSB at the *S1hygro* gene could be assayed by selecting for hygromycin-resistant cell clones and physically analyzing the repair products by genomic DNA blotting or by direct PCR followed by digestion with *Nco*I endonuclease. Using a similar system, the Ku80 protein has been demonstrated to be crucial for NHEJ of a defined chromosomal DSB *in vivo* (32).

The *S1hygro* DSB repair substrate containing a puromycin selection cassette was stably integrated into the genome of wild-type, *p53*$^{-/-}$, and *Brca1*$^{-/-}$:*p53*$^{-/-}$ MEFs by either plasmid transfection or retroviral infection. Puromycin-resistant clones were selected and analyzed by Southern blotting and PCR. MEF clones containing a single copy of *S1hygro* were chosen for the chromosomal DSB-promoted NHEJ repair assay as described above. To generate DSBs, I-*Sce*I endonuclease was introduced by transfection of an I-*Sce*I expression vector (33) into the MEFs. In the mock transfection experiment, few or no hygromycin-resistant colonies were obtained following a selection against hygromycin. However, expression of the I-*Sce*I endonuclease in either the wild-type or the *p53*$^{-/-}$ MEFs pro-

TABLE I
Brca1 promotes NHEJ of Chromosomal DSBs
1×10^6 cells were used in each assay.

Cell line	No. of Hygro^r colonies[a]		
	Genotype	Mock-transfected	I-*Sce*I
WT-1	Wild type	1 ± 1	50 ± 3
p53-3	$p53^{-/-}Brca1^{+/+}$	<1	86 ± 19
p53-4	$p53^{-/-}Brca1^{+/+}$	<1	90 ± 16
1H-5	$p53^{-/-}Brca1^{-/-}$	<1	<1
	Number of Hygro^r colonies[b]		
	Genotype	Mock-transfected	I-*Sce*I
RP-3	$p53^{-/-}Brca1^{+/+}$	<1	45 ± 17
RP-4	$p53^{-/-}Brca1^{+/+}$	<1	82 ± 41
RP-6	$p53^{-/-}Brca1^{+/+}$	<1	45 ± 15
RH-1	$p53^{-/-}Brca1^{-/-}$	<1	<1
RH-3	$p53^{-/-}Brca1^{-/-}$	<1	1 ± 1
RH-6	$p53^{-/-}Brca1^{-/-}$	<1	<1

[a] 1–2 copies of *S1hygro* were introduced into the cells by plasmid transfection.
[b] Single copies of *S1hygro* were introduced into the cells by retroviral DNA integration.

duced numerous hygromycin-resistant colonies (Fig. 4*B* and Table I), indicating that I-*Sce*I cleavage occurred at the *S1hygro* substrate and hygromycin resistance arose almost exclusively from the repair of the I-*Sce*I-cleaved substrates. These results demonstrate that a defined chromosomal DSB can stimulate NHEJ as much as 100-fold above the spontaneous level.

Expression of I-*Sce*I in either wild-type or $p53^{-/-}$ MEFs yielded 45–82 hygromycin-resistant colonies/10^6 cells (4.5×10^{-5}-8.2×10^{-5}). By contrast, only background levels of hygromycin-resistant colonies were obtained after transfection of I-*Sce*I in *Brca1* $^{-/-}$:$p53^{-/-}$ MEFs (Table I). The transfection efficiency of the parental *Brca1* $^{-/-}$:$p53^{-/-}$ MEF was 2-fold lower than *Brca1* wild-type cells. However, each individual clone harboring *S1hygro* had a varied transfection efficiency of between 2-fold lower (RH3) to 3-fold higher (RH1) when compared with the clones derived from *Brca* $^{+/+}$:$p53^{-/-}$ MEF (RP3 and RP4), as measured by a transient transfection assay with a SV40 promoter-driven luciferase reporter (data not shown). Only background levels of hygromycin-resistant colonies were formed in a *Brca1* $^{-/-}$:$p53^{-/-}$ MEF clone (RH1) despite its highest transfection efficiency. Therefore, mutation of *Brca1* decreased the formation of hygromycin-resistant colonies by 1–2 orders of magnitude.

The repair of DSBs by NHEJ in the hygromycin-resistant clones would be expected to restore the naturally occurring *Nco*I restriction site, which was destroyed by the insertion of the 18-bp I-*Sce*I recognition site during construction of the *S1hygro* substrate. To verify that the hygromycin-resistant colonies derived from I-*Sce*I-induced DSB repair did in fact arise from NHEJ, a 595-bp DNA fragment of the hygromycin resistance gene encompassing the inactivated *Nco*I and I-*Sce*I restriction sites was amplified by PCR and subjected to *Nco*I restriction enzyme digestion (Fig. 4*C*). Nine of 10 PCR products generated from the hygromycin-resistant colonies were completely cleaved by *Nco*I but were resistant to I-*Sce*I digestion. In contrast, PCR products derived from parental clones harboring *S1hygro* were readily cleaved by I-*Sce*I but not by *Nco*I (Fig. 4*D*). These results indicated that cleavage followed by end processing must have occurred in these cells to restore the *Nco*I site.

To ensure a high level of I-*Sce*I expression, an adenovirus, AdTrack-CMV-I-*Sce*I, encoding I-*Sce*I and GFP under two distinct promoters was generated (Fig. 5*A*). We then tested this

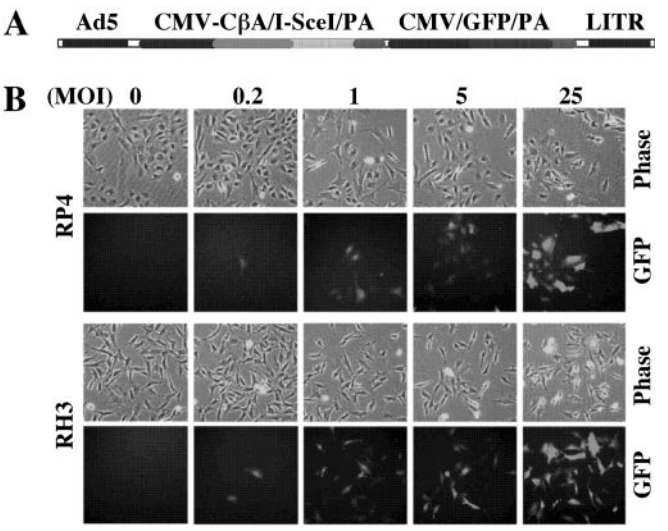

C

Genotype	Number of Hygro^r colonies			
	p53-/-Brca1+/+		*p53-/-Brca1-/-*	
Cell line	RP3	RP4	RH1	RH3
MOI				
Adeno-GFP 25	<1	<1	<1	<1
Adeno-I-SceI				
0.2	2±2	3±1	<1	<1
1	13±4	15±1	<1	1±1
5	35±4	51±5	<1	<1
25	77±7	124±7	<1	<1

FIG. 5. **Efficient expression of I-*Sce*I delivered by adenovirus enhances NHEJ.** *A*, diagram of the adenovirus construct AdTrack-CMV-I-*Sce*I, which contains two distinct expression units for I-*Sce*I under the CMV-CβA promoter (a composite promoter of cytomegalovirus (*CMV*) late gene promoter and chicken β-actin promoter) and for GFP under the CMV promoter. About 2×10^5 Brca1-proficient (RP3 and RP4) or -deficient cells (RH1 and RH3) were infected with the adenovirus AdTrack-CMV-I-*Sce*I at different m.o.i. dosages. *B*, as an example of RH3 and RP4, the number of the GFP-positive cells was proportional to the m.o.i. level as indicated. Cells expressing GFP fluorescence were recorded 48 h post-infection (magnification, 400×). *C*, the corresponding infected cells were grown in medium containing hygromycin for 14 days. As indicated, the number of hygromycin-resistant colonies increased proportionally to the m.o.i. level in RP3 and RP4 but was undetectable in RH3 and RH1 MEFs. Infection with Adeno-I-GFP that expressed only GFP alone did not increase any hygromycin-resistant colonies in either type of MEF.

adenovirus over a series of m.o.i. by tracing the fluorescence derived from GFP to monitor the infection efficiency. As shown in Fig. 5*B*, the expression of GFP in *Brca1* mutant or wild-type MEFs was comparable following the infection of AdTrack-CMV-I-*Sce*I in the range of m.o.i. used, suggesting that there was no significant difference between these two MEFs in terms of adenovirus infection and expression. We observed that the hygromycin-resistant colonies increased in proportion to the amount of m.o.i. infected in *Brca1*$^{+/+}$:$p53^{-/-}$ MEFs compared with *Brca1* $^{-/-}$:$p53^{-/-}$ MEFs, which remained negligible regardless of the high m.o.i. used (Fig. 5*C*). Taken together, these results suggested that the Brca1 mutant cells exhibited a severe defect in the repair of DSBs by microhomology-mediated NHEJ.

To establish that the above described microhomology-mediated end joining preceded independent of drug selection, we examined the repair process of the *S1hygro* substrate in these MEFs upon expression of the I-*Sce*I endonuclease at earlier

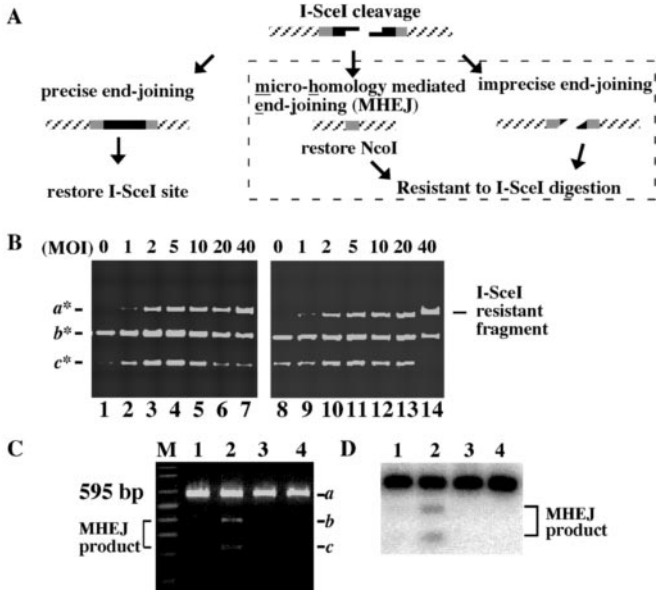

FIG. 6. **Analysis of earlier time points for chromosomal end joining induced by I-*Sce*I DSBs by transient transfection.** *A*, illustration of the potential processes for repairing I-*Sce*I-induced DSB and the properties of the end products derived from each repair process. The first pathway is mediated by a precise end joining that will regenerate the I-*Sce*I site; its end product is indistinguishable from the original substrate. This pathway cannot be analyzed by this method. The second pathway functions through MHEJ, which restores the *Nco*I site. The third pathway is mediated by imprecise end joining, and the end product loses the I-*Sce*I site and does not restore the *Nco*I site. *B*, physical analysis of the nonhomologous end-joining product. Genomic DNA from RP3 (*Brca1*$^{+/+}$:*p53*$^{-/-}$, *lanes 1–7*) or RH1 (*Brca1*$^{-/-}$:*p53*$^{-/-}$, *lanes 8–14*) MEFs infected with different m.o.i. of AdTrack-CMV-I-*Sce*I as indicated were used as templates to generate 573–595-bp PCR fragments as described in Fig 4. The PCR products were digested with I-*Sce*I endonuclease, separated by agarose gel electrophoresis, and stained with ethidium bromide. The presence of the I-*Sce*I-resistant DNA fragments (*a**) in both cell types indicates that they have similar efficiencies in NHEJ after I-*Sce*I expression. *C*, physical analysis of microhomology-mediated end-joining products. Genomic DNA from RP3 (*Brca1*$^{+/+}$:*p53*$^{-/-}$, *lanes 1* and *2*) or RH1 (*Brca1*$^{-/-}$:*p53*$^{-/-}$, *lanes 3* and *4*) MEFs infected with 20 m.o.i. of AdTrack-CMV-I-*Sce*I (*lanes 2* and *4*) or Adeno-I-GFP (*lanes 1* and *3*) were used as templates to generate the PCR fragments as described above. The PCR products (*lanes 2* and *4*) were digested with *Nco*I endonuclease, analyzed by agarose gel electrophoresis, and stained with ethidium bromide. *Lane M* shows the DNA size marker. The appearance of two DNA fragments (*b* and *c*) from *Nco*I digestion (*lane 2*) indicates the presence of the recovered *Nco*I site through microhomology-mediated end joining. *D*, DNA blotting analysis using hygromycin resistance gene cDNA as probe. The gel shown in *C* was analyzed by Southern blotting with p32-labeled cDNA of the hygromycin resistance gene as described (21).

time points. These *Brca1*$^{+/+}$:*p53*$^{-/-}$ and *Brca1* $^{-/-}$:*p53*$^{-/-}$ MEFs were infected with different m.o.i. levels of the adenovirus, AdTrack-CMV-I-*Sce*I, for 36 h. To demonstrate that I-*Sce*I endonuclease was expressed efficiently in both cell types, the genomic DNA of these cells was extracted, and the 595-bp hygromycin DNA fragment was amplified by PCR. The resistance of the 595-bp hygromycin DNA fragment to I-*Sce*I digestion indicates that a NHEJ must occur after I-*Sce*I cleavage. As shown in Fig. 6*B*, the I-*Sce*I-resistant fragment appeared in both Brca1-proficient and -deficient MEFs with very similar kinetics. This result also suggested that a deficiency of Brca1 did not affect the overall NHEJ activity. If NHEJ was to proceed through the designed CATG microhomology, the resulting repair product could be cleaved by the *Nco*I restriction enzyme as described above (Fig. 6*A*). Consistent with our previous observation, a portion of the NHEJ proceeded through the CATG microhomology, thereby restoring the original *Nco*I site in the *Brca1* wild-type cells. Therefore, the 595-bp hygromycin

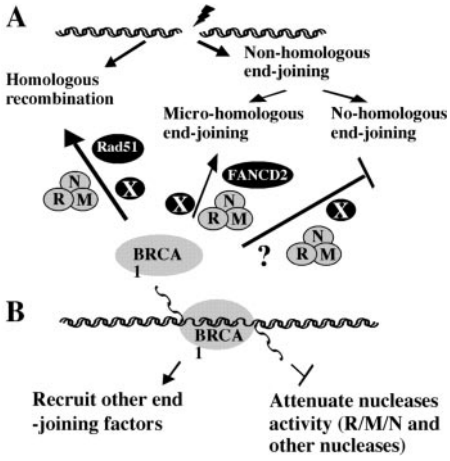

FIG. 7. **Proposed multiple functions of BRCA1 in DNA double strand break repair.** *A*, BRCA1 is important in homology-based repair and microhomology-mediated end joining, possibly through its direct interaction with the Rad50·Mre11·Nbs1 complex (*R/M/N*), and/or indirect association with Rad51, and/or other unknown factors (*X*). BRCA1 may also function in the suppression of nonhomologous end joining through Rad50·Mre11·Nbs1 or other proteins. *B*, BRCA1 may bind to a microhomology-paired double-stranded DNA to stabilize it transiently before recruiting other repair factors involved in further processing.

DNA fragment derived from genomic PCR could be cleaved by *Nco*I into two fragments, as either directly revealed by ethidium bromide staining (Fig. 6*C*) or by DNA blotting using the cDNA of the hygromycin resistance gene as a probe (Fig. 6*D*). This type of NHEJ activity was readily detectable in the Brca1-proficient MEFs but not in Brca1-deficient cells (Fig. 6, *C* and *D*). Taken together, these results suggest that Brca1 plays an important role in microhomology-mediated end-joining activity in the repair of DNA DSBs *in vivo*.

DISCUSSION

BRCA1 plays an essential role in DNA DSB repair either through HR or NHEJ. The results described above suggest that Brca1 may have an important role in NHEJ. Using a plasmid end-joining assay, it was shown that Brca1 plays a moderate role in precise end joining rather than in overall NHEJ. Brca1 was also found to promote efficient retroviral infection, likely reflecting a role in retroviral DNA end-joining activity. Furthermore, repair of a defined chromosomal DSB mediated by microhomology annealing is severely impaired in Brca1-deficient MEFs. Taken together, these observations suggest that BRCA1 has a critical role in microhomology-mediated end joining rather than in overall nonhomologous end-joining activity. These results are consistent with the recent observation that cell extracts derived from Brca1-deficient MEFs significantly reduced end-joining activity with 4-bp homology *in vitro* (34).

Mechanistically speaking, NHEJ can proceed through distinct subpathways determined by the nucleotide sequence immediately surrounding the break site. Often, NHEJ generates junctions with sequence homologies consisting of only a few nucleotides. DNA ends can be joined either precisely, without nucleotide loss through sequence homology at the DNA termini, or imprecisely, through nucleotide deletion or addition, to generate microhomologies flanking the break site. Alternatively, broken DNA ends can be joined without microhomology (15). In an assay for gross chromosomal rearrangements (GCRs), the rate of non-homology-mediated GCRs was increased ~600-fold in yeast *rad50, mre11,* and *xrs2* mutants (35), suggesting that the Rad50·Mre11·Xrs2 complex appears to be important in suppressing non-homology-mediated end-joining processes. Previous work has demonstrated that BRCA1

physically interacts with the Rad50·Mre11·Nbs1 complex *in vivo* and *in vitro* (14). Furthermore, BRCA1 can be isolated from cells in a high molecular complex with Rad50·Mre11·Nbs1 (36). These observations suggest that the function of BRCA1 in DSB repair is mediated, at least in part, through its association with the Rad50·Mre11·Nbs1 complex (Fig. 7*A*), although the possibility exists that BRCA1 functions through other associated repair component such as FANCD2 (37, 38).

The function of the mammalian Rad50·Mre11·Nbs1 complex in DSB repair is not entirely known at present. However, substantial evidence has suggested a functional conservation between the mammalian Rad50·Mre11·Nbs1 and yeast Rad50·Mre11·Xrs2 in NHEJ. It has been shown that the yeast Rad50·Mre11·Xrs2 purified complex can bind and bridge DNA ends together. The addition of the yeast homologues of Ku70/80, HdfA and HdfB, enhances this DNA end-bridging activity of the Rad50·Mre11·Xrs2 complex. The DNA-bound Rad50·Mre11·Xrs2 complex can then directly recruit Dnl4/Lif1 (equivalent to mammalian DNA ligase IV and Xrcc4) to complete the DNA end ligation process (40). Similarly, mammalian Rad50·Mre11·Nbs1 has also been to exhibit DNA end-tethering activity (39, 41, 42). Therefore, purified proteins that include Rad50·Mre11·Nbs1, Ku homologues, and DNA ligase IV/Xrcc4 can carry out NHEJ *in vitro*. These results implicate a potential conservation of these two complexes in nonhomologous end joining.

The NHEJ pathway represents an efficient, energy-saving process to rescue cells following extensive DNA damage. NHEJ can be error-prone in mammalian cells. However, NHEJ may utilize microhomology sequences to minimize error rates. If complimentary sequences are left at the DNA termini, these DNA termini can be joined readily without nucleotide loss by annealing the complementary sequences. Experimental evidence has suggested that this type of error-free NHEJ could represent up to 60% of overall end joining in mammalian cells (17) and more than 90% in yeast when a cohesive overhang is present at the DNA termini (15). On the other hand, microhomology sequences may serve as a platform for stabilizing protein-DNA interactions, attenuating nuclease attack, recruiting other repair factors, and bridging DNA ends together (Fig. 7*B*). BRCA1 has been shown to associate with this type of DNA structure *in vitro*, suggesting that BRCA1 may participate in this process (38). Similar models have been proposed for DNA-PK through structural analytical studies (43, 44). Proper NHEJ contributes significantly to maintain genome stability in mammalian cells. It has been demonstrated that in the presence of multiple chromosomal breaks, homology-directed translocation can be observed at a frequency as high as that of conservative gene conversion (45). In the absence of DNA-PK or ligase IV/Xrcc4, greatly elevated levels of chromosomal translocation can be detected in murine embryonic cells (10–12).

As discussed above, Brca1 may work together with the Rad50·Mre11·Nbs1 complex in NHEJ in addition to homologous recombination. The timing for this complex to function in either pathway may be dependent on the cell cycle status, at which the availability of the other repair factors of these two pathways is critical. Inefficient or error-prone DNA repair resulting directly from mutational inactivation of BRCA1 can lead to global genomic instability and a concomitant accrual of functionally inactivating mutations at genetic loci involved in breast tumorigenesis.

Acknowledgments—We thank Drs. P. Berg and G. Donoho for pPGK3Xnls-I-*Sce*I plasmid, P. Hasty for *Ku* mutant MEFs, N. Ting and S. Vijayakumar for comments, and D. Jones for technical assistance.

REFERENCES

1. Welcsh, P. L., Owens, K. N., and King, M. C. (2000) *Trends Genet.* **16,** 69–74
2. Zheng, L., Li, S., Boyer, T. G., and Lee, W. H. (2000) *Oncogene* **19,** 6159–6175
3. Tomlinson, G. E., Chen, T.-L., Stastny, V. A., Virmani, A. K., Spillman, M. A., Tonk, V., Blum, J. L., Schneider, N. R., Wistuba, I. I., Shay, J. W., Minna, J. D., and Gazdar, A. F. (1998) *Cancer Res.* **58,** 3237–3242
4. Xu, X., Weaver, Z., Linke, S. P., Li, C., Gotay, J., Wang, X. W., Harris, C. C., Ried, T., and Deng, C. X. (1999) *Mol. Cell* **3,** 389–395
5. Gowen, L. C., Avrutskaya, A. V., Latour, A. M., Koller, B. H., and Leadon, S. A. (1998) *Science* **281,** 1009–1012
6. Cressman, V. L., Backlund, D. C., Avrutskaya, A. V., Leadon, S. A., Godfrey, V., and Koller, B. H. (1999) *Mol. Cell. Biol.* **19,** 7061–7075
7. Deng, C. X. (2001) *Mutat. Res.* **477,** 183–189
8. Chu, G. (1997) *J. Biol. Chem.* **272,** 24097–24100
9. Roth, D. B., and Gellert, M. (2000) *Nature* **404,** 823–825
10. Karanjawala, Z. E., Grawunder, U., Hsieh, C. L., and Lieber, M. R. (1999) *Curr. Biol.* **9,** 1501–1504
11. Difilippantonio, M. J., Zhu, J., Chen, H. T., Meffre, E., Nussenzweig, M. C., Max, E. E., Ried, T., and Nussenzweig, A. (2000) *Nature* **404,** 510–514
12. Gao, Y., Ferguson, D. O., Xie, W., Manis, J. P., Sekiguchi, J., Frank, K. M., Chaudhuri, J., Horner, J., DePinho, R. A., and Alt, F. W. (2000) *Nature* **404,** 897–900
13. Lim, D. S., Vogel, H., Willerford, D. M., Sands, A. T., Platt, K. A., and Hasty, P. (2000) *Mol. Cell. Biol.* **20,** 3772–3780
14. Zhong, Q., Chen, C. F., Li, S., Chen, Y., Wang, C. C., Xiao, J., Chen, P. L., Sharp, Z. D., and Lee, W. H. (1999) *Science* **285,** 747–750
15. Tsukamoto, Y., and Ikeda, H. (1998) *Genes Cells* **3,** 135–144
16. Moynahan, M. E., Chiu, J. W., Koller, B. H., and Jasin, M. (1999) *Mol. Cell* **4,** 511–518
17. Lin, Y., Lukacsovich, T., and Waldman, A. S. (1999) *Mol. Cell. Biol.* **19,** 8353–8360
18. Takata, M., Sasaki, M. S., Sonoda, E., Morrison, C., Hashimoto, M., Utsumi, H., Yamaguchi-Iwai, Y., Shinohara, A., and Takeda, S. (1998) *EMBO J.* **17,** 5497–5508
19. Scully, R., Ganesan, S., Vlasakova, K., Chen, J., Socolovsky, M., and Livingston, D. M. (1999) *Mol. Cell* **4,** 1093–1099
20. Pierce, A. J., Stark, J. M., Araujo, F. D., Moynahan, M. E., Berwick, M., and Jasin, M. (2001) *Trends Cell Biol.* **11,** S52–S59
21. Liu, C. Y., Flesken-Nikitin, A., Li, S., Zeng, Y. Y., and Lee, W. H. (1996) *Genes Dev.* **10,** 1835–1843
22. Zheng, L., Pan, H., Li, S., Flesken-Nikitin, A., Chen, P. L., Boyer, T. G., and Lee, W. H. (2000) *Mol. Cell* **6,** 757–768
23. Donehower, L. A., Harvey, M., Slagle, B. L., McArthur, M. J., Montgomery, C. A., Jr., Butel, J. S., and Bradley, A. (1992) *Nature* **356,** 215–221
24. He, T. C., Zhou, S., da Costa, L. T., Yu, J., Kinzler, K. W., and Vogelstein, B. (1998) *Proc. Natl. Acad. Sci. U. S. A.* **95,** 2509–2514
25. Chen, P. L., Chen, Y. M., Bookstein, R., and Lee, W. H. (1990) *Science* **250,** 1576–1580
26. Pear, W. S., Nolan, G. P., Scott, M. L., and Baltimore, D. (1993) *Proc. Natl. Acad. Sci. U. S. A.* **90,** 8392–8396
27. Gowen, L. C., Johnson, B. L., Latour, A. M., Sulik, K. K., and Koller, B. H. (1996) *Nat. Genet.* **12,** 191–194
28. Huber, L. J., Yang, T. W., Sarkisian, C. J., Master, S. R., Deng, C. X., and Chodosh, L. A. (2001) *Mol. Cell. Biol.* **21,** 4005–4015
29. Hakem, R., de la Pompa, J. L., Elia, A., Potter, J., and Mak, T. W. (1997) *Nat. Genet.* **16,** 298–302
30. Daniel, R., Katz, R. A., and Skalka, A. M. (1999) *Science* **284,** 644–647
31. Li, L., Olvera, J. M., Yoder, K. E., Mitchell, R. S., Butler, S. L., Lieber, M., Martin, S. L., and Bushman, F. D. (2001) *EMBO J.* **20,** 3272–3281
32. Liang, F., Romanienko, P. J., Weaver, D. T., Jeggo, P. A., and Jasin, M. (1996) *Proc. Natl. Acad. Sci. U. S. A.* **93,** 8929–8933
33. Donoho, G., Jasin, M., and Berg, P. (1998) *Mol. Cell. Biol.* **18,** 4070–4078
34. Zhong, Q., Boyer, T. G., Chen, P.-L., and Lee, W.-H. (2002) *Cancer Res.*, in press
35. Chen, C., and Kolodner, R. D. (1999) *Nat. Genet.* **23,** 81–85
36. Chiba, N., and Parvin, J. D. (2001) *J. Biol. Chem.* **276,** 38549–38554
37. Garcia-Higuera, I., Taniguchi, T., Ganesan, S., Meyn, M. S., Timmers, C., Hejna, J., Grompe, M., and D'Andrea, A. D. (2001) *Mol. Cell* **7,** 249–262
38. Lundberg, R., Mavinakere, M., and Campbell, C. (2001) *J. Biol. Chem.* **276,** 9543–9549
39. Paull, T. T., and Gellert, M. (2000) *Proc. Natl. Acad. Sci. U. S. A.* **97,** 6409–6414
40. Chen, L., Trujillo, K., Ramos, W., Sung, P., and Tomkinson, A. E. (2001) *Mol. Cell* **8,** 1105–1115
41. Huang, J., and Dynan, W. S. (2002) *Nucleic Acids Res.* **30,** 667–674
42. de Jager, M., van Noort, J., van Gent, D. C., Dekker, C., Kanaar, R., and Wyman, C. (2001) *Mol. Cell* **8,** 1129–1135
43. Leuther, K. K., Hammarsten, O., Kornberg, R. D., and Chu, G. (1999) *EMBO J.* **18,** 1114–1123
44. Walker, J. R., Corpina, R. A., and Goldberg, J. (2001) *Nature* **412,** 607–614
45. Richardson, C., and Jasin, M. (2000) *Nature* **405,** 697–700